DNS OF TURBULENT HEAT TRANSFER IN A CHANNEL FLOW WITH STREAMWISELY VARYING THERMAL BOUNDARY CONDITION

Yohji Seki, Hiroshi Kawamura
Department of Mechanical Engineering,
Tokyo University of Science
2641 Yamazaki, Noda-shi, Chiba 278-8510, Japan
a7598074@rs.noda.tus.ac.jp, kawa@rs.noda.tus.ac.jp

ABSTRACT

The direct numerical simulation (DNS, hereafter) of turbulent heat transfer in a fully developed turbulent channel flow has been carried out for streamwisely varying thermal boundary condition ($Re_\tau = 180$) with $Pr = 0.71$ to obtain the statistical mean temperature, the temperature variance, their budget terms and the time scale ratio etc. The present results have indicated that the time scale ratio and the turbulent Prandtl number vary along a streamwise direction. Therefore, the turbulent Prandtl number cannot be used for the estimation of the turbulent heat flux in the case of thermal boundary condition with rapid streamwise variation. The counter gradient diffusion takes place near the heated wall and downstream.

INTRODUCTION

With the aid of recent developments in super and parallel computers, the DNS of turbulent flow is now often performed. The DNS is able to provide with a large amount of detailed data on the turbulent heat transfer with various thermal boundary conditions. Several experiments (Johnson, 1959 and Antonia et al., 1977) and turbulent modelling studies (Nagano et al., 1995) for the streamwisely varying thermal boundary conditions were carried out in the past studies. However, no DNS has been done for streamwisely varying thermal boundary condition.

The present study aims to obtain the distribution of various thermal statistics by DNS of the turbulent channel flow and also to examine the turbulent scalar transport quantities in detail with the streamwisely varying thermal boundary condition.

NUMERICAL PROCEDURE

The DNS of turbulent heat transfer in a fully developed turbulent channel flow has been carried out for streamwisely varying thermal boundary condition with $Pr = 0.71$ and $Re_\tau = 180$, based on the friction velocity u_τ and channel half width δ, and $Re_c = 6600$, based on the center velocity u_c and 2δ. The computational domain is given in Fig. 1. The computational domain is divided into three parts; the entrance region, the test region and the cooling (fringe) region. In the fringe region, an extra damping function is added in the energy equation to attenuate the temperature. Thus the periodic boundary condition can be applied in the streamwise direction with maintaining the inlet temperature being zero. The buoyancy effect is not taken into consideration to examine the fundamental nature of the convective turbulent heat transfer in this research.

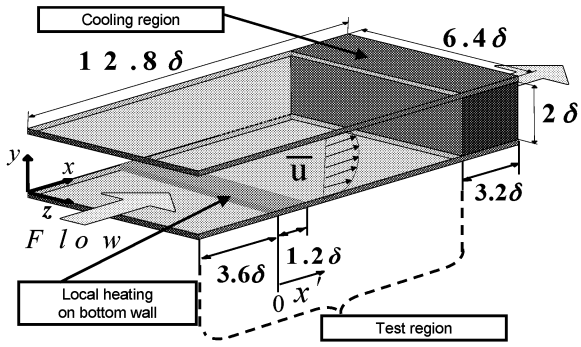

Figure 1: Configuration.

The coordinates and flow variables are normalized by the channel half width δ, the kinematic viscosity ν, the friction velocity u_τ, and the maximum temperature on the bottom wall T_{max}. The fundamental equations are the continuity equation:

$$\frac{\partial u_i^+}{\partial x_i^*} = 0, \tag{1}$$

and the Navier-Stokes equation:

$$\frac{\partial u_i^+}{\partial t^*} + u_j^+ \frac{\partial u_i^+}{\partial x_j^*} = -\frac{\partial p^+}{\partial x_i^*} + \frac{1}{Re_\tau}\frac{\partial^2 u_i^+}{\partial x_j^{*2}} + \frac{d\bar{p}^+}{dx_1^*}\delta_{i1}. \tag{2}$$

Here, $i = 1$, 2 and 3 indicate the streamwise, wall-normal and spanwise directions, respectively. The variables t and p are the time and the pressure, respectively. Variables with the superscript $+$ and $*$ indicate those normalized by wall units and the channel half width δ, respectively. The third term in the right-hand side of Eq. (2) is the streamwise mean pressure gradient. The boundary condition for the momentum field is

$$u_i^+ = 0, \qquad \text{at } y = 0 \text{ and } 2\ \delta. \tag{3}$$

The enegy equation for the instantaneous temperature $T^+(x^*, y^*, z^*)$ is expressed as

$$\frac{\partial T^*}{\partial t^*} + u_j^+ \frac{\partial T^*}{\partial x_j^*} = \frac{1}{Re_\tau \cdot Pr}\frac{\partial^2 T^*}{\partial x_j^{*2}} - Q(x). \tag{4}$$

The endothermal term ($Q(x) = \lambda(x)T^*$) is non-zero only in the fringe (cooling) region, where the fringe function $\lambda(x)$ is

Table 1: Computational conditions.

$L_x \times L_y \times L_z$	$N_x \times N_y \times N_z$	Δx^+	Δy^+	Δz^+
$12.8\delta \times 2\delta \times 6.4\delta$	512×128×256	4.5	0.2∼5.9	4.5

the strength of the heat sink with a maximum of inverse number of the time step Δt^{*-1}. The form of $\lambda(x)$ is designed to minimize the upstream temperature influence. The heating condition at the bottom wall is

$$T_{wall}(\xi) = T_{\max} \cdot \sin^2(\pi\xi)$$
$$if \;\; 0 \le \xi \le 1, \quad else \;\; T_{wall}(\xi) = 0 \;\; \text{at } y = 0,$$
$$where \quad \xi = x'/D_L, \quad x' = x - 3D_L, \tag{5}$$

where D_L is the heated streamwise length of 1.2δ. Figure 2 shows the thermal boundary condition given by Eq. (5) at the bottom wall. On the other hand, the thermal boundary condition at the top wall is assigned to be zero.

Statistic quantities are taken to the spanwise direction and the time step. The simulation has been made with the use of the finite difference method in which special attention is paid to the consistency between the analytical and numerical differential operations (Kawamura, 1994). The method was confirmed to give good agreement with the spectral method (Kawamura and Kondoh, 1996). This consistency with the analytical operation ensures the balance of the transport equations for the statistical correlations such as the temperature variance and the turbulent heat flux. A fourth-order central difference scheme is adopted in the streamwise and spanwise directions, and the second-order central difference scheme is used in the wall-normal direction. Further details of the method can be found in Abe et al. (2001), Kawamura (1994), and Kawamura and Kondoh (1996). The computational condition is shown in table 1. The computation has been performed with the use of 8 processing elements of VPP5000.

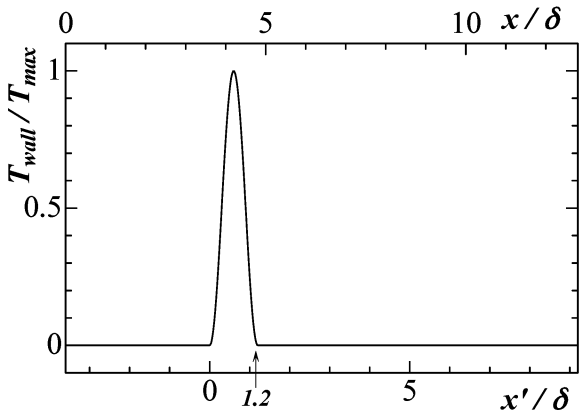

Figure 2: Variation of bottom wall temperature.

RESULTS AND DISCUSSION

Mean temperature profiles are shown in Fig. 3. If the maximum temperature (above ambient) T_γ and the wall-normal distance γ of $T/T_\gamma = 0.5$ are chosen as the temperature and length scales respectively, the values of DNS (upstream of $x'/\delta = 0.8$) are similar to experimental data (Sreenivasan et al., 1976) of heated wall-Cylinder immersed in a turbulent boundary layer. The mean temperature gradient becomes the plus in downstream of $x'/\delta = 1.0$ because of a rapid reduction of wall-temperature. Moreover, the peak of the mean temperature is maintained at $y/\gamma = 0.5$ independent of the downstream position in case of this normalization.

Figs. 4 and 5 show the turbulent heat flux $\overline{u'^+\theta'^*}$ and $\overline{v'^+\theta'^*}$

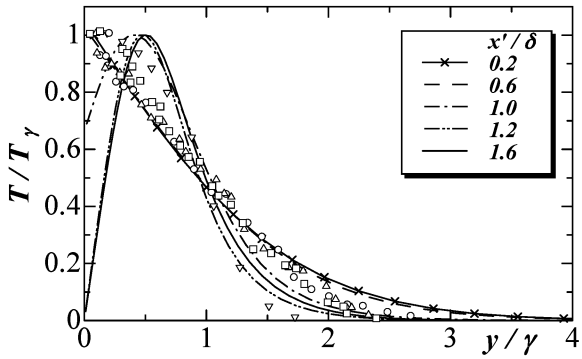

Figure 3: Mean temperature, symbols are experimental data (Sreenivasan et al., 1976), ▽:$x' = 9.6$, △:$x' = 37.2$, ○:$x' = 75.6$, □:$x' = 122.4$.

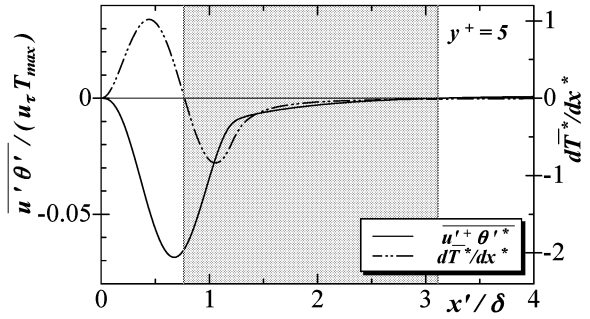

Figure 4: Streamwise turbulent heat flux; $\overline{u'^+\theta'^*}$.

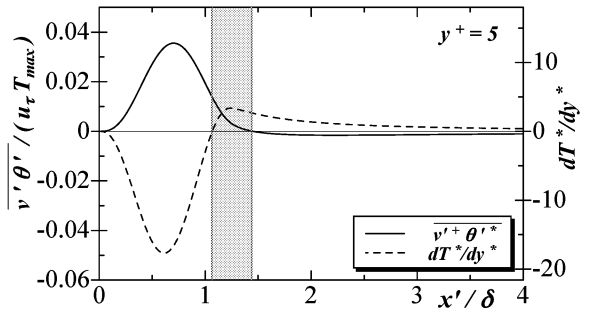

Figure 5: Spanwise turbulent heat flux; $\overline{v'^+\theta'^*}$.

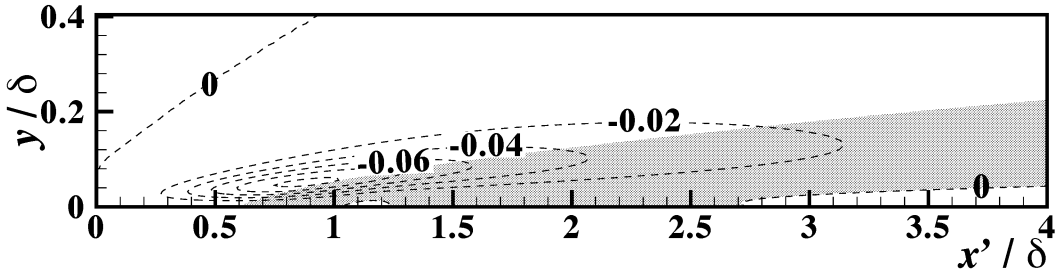

Figure 6: Contour of the turbulent heat flux $\overline{u'^+\theta'^*}$ (dot line). The gray region presents the counter gradient diffusion in which both the negative turbulent heat flux $\overline{u'^+\theta'^*}$ and the negative mean temperature gradient $d\bar{T}^*/dx^*$ exist.

in the near wall region, respectively. The mean temperature gradients are also plotted in these figures. The sign of the turbulent heat flux is usually opposite to the temperature gradient. This relation can be written as:

$$-\quad \overline{u_i'^+\theta'^*} \quad = \quad \kappa_t \quad \times \quad d\bar{T}^*/dx_i^*, \tag{6}$$

where κ_t is thermal eddy diffusivity. In the gray region of Fig. 4, however, $\overline{u'^+\theta'^*}$ is still negative despite negative temperature gradient $d\bar{T}^*/dx^*$. This indicates that the counter gradient diffusion takes place in the gray region. The counter gradient diffusion exists for $\overline{u'^+\theta'^*}$ behind $x'/\delta = 0.8$ at the $y^+ = 5$. The counter gradient diffusion is observed behind $x'/\delta = 1.1$ for $\overline{v'^+\theta'^*}$ at the $y^+ = 5$ as well. Figure 6 shows the two dimensional distribution for $\overline{u'^+\theta'^*}$. The gray represents the region where the turbulent heat flux $\overline{u'^+\theta'^*}$ and the mean temperature gradient $d\bar{T}^*/dx^*$ are both negative.

Turbulent Prandtl number

The turbulent Prandtl number Pr_t, defined as the ratio of momentum diffusivity to thermal diffusivity, i.e.,

$$Pr_t \equiv \frac{\overline{u'^+v'^+}}{\overline{v'^+\theta'^*}} \frac{d\bar{T}^*/dy^+}{d\bar{u}^+/dy^+}. \tag{7}$$

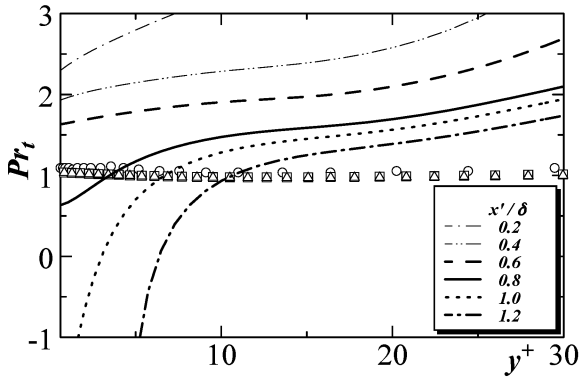

Figure 7: Turbulent Prandtl number, ○:Uniform heat source (Antonia and Kim, 1991), △:Constant wall temperature difference (Seki et al., 2003), □:Uniform heat flux heating (Seki et al., 2003).

Figure 7 shows Pr_t evaluated from the present data at several stations. The calculated result (Antonia and Kim, 1991) for uniform heat source is also plotted in Fig. 7. The other calculated results of the constant wall temperature difference and the uniform heat flux heating by authors' group (Seki et al., 2003) are also plotted in Fig. 7. In most of the existing studies, Pr_t tends to be a constant value of 1.0 for several thermal boundary conditions (Antonia and Kim, 1991; Seki et al., 2003). In the case of the present streamwisely varying thermal boundary condition, however, Fig. 7 shows that Pr_t is totally different than the constant value of 1.0. This tendency is qualitatively similar to the one reported by Antonia et al. (1977). Especially, in the near-wall region, Pr_t becomes negative downstream. The sign of Pr_t related with the turbulent heat-flux and temperature gradient can be obtained through the following relation:

$$Pr_t \equiv \frac{\overline{u'^+v'^+}}{\overline{v'^+\theta'^*}} \cdot \frac{d\bar{T}^*/dy^+}{d\bar{u}^+/dy^+} = \frac{- \cdot +}{+ \cdot +} = -. \tag{8}$$

Thus, this result correlates well with counter gradient diffusion.

Turbulent Prandtl number Pr_t is often used to obtain the turbulent heat flux from the mean temperature gradient. Figure 7, however, indicates that it cannot be used for the estimation of the turbulent heat flux in case of the thermal boundary condition with rapid streamwise variation since Pr_t changes significantly along the streamwise direction.

Time scale ratio

The time scale ratio R is expressed as the ratio of the scalar time scale $\tau_\theta (= k_\theta/\varepsilon_\theta)$ to the momentum one $\tau_u (= k/\varepsilon)$;

$$R = \frac{\tau_\theta}{\tau_u} = \frac{k_\theta}{\varepsilon_\theta} \frac{\varepsilon}{k}. \tag{9}$$

Because the velocity field is the fully developed turbulent channel flow in this study, the momentum time scale $\tau_u (= k/\varepsilon)$ is constant along the streamwise direction. Therefore, the scalar time scale $\tau_\theta (= k_\theta/\varepsilon_\theta)$ determines R along the streamwise direction:

$$R \propto \tau_\theta = \frac{k_\theta}{\varepsilon_\theta}. \tag{10}$$

Figure 8 shows the distribution of the time scale ratio. The wall-asymptotic value of R is analytically equal to the molecular Prandtl number. The near-wall limiting value of R given

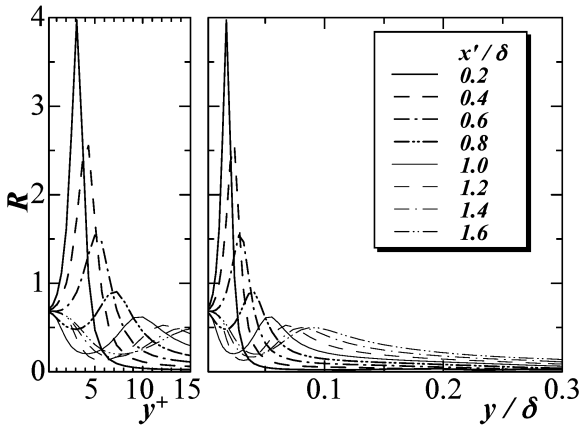

Figure 8: Time scale ratio.

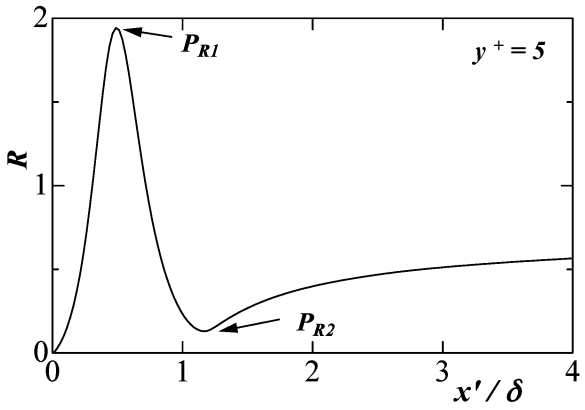

Figure 10: Time scale ratio at the inner region.

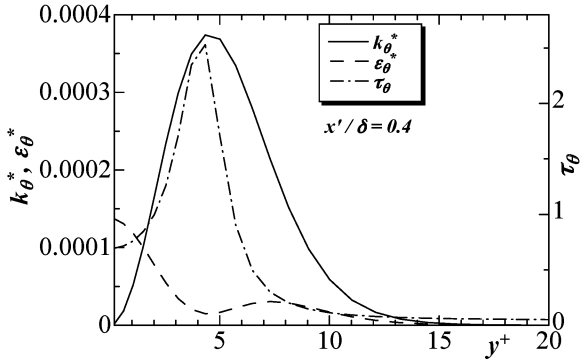

Figure 9: k_θ^* and its dissipation rate.

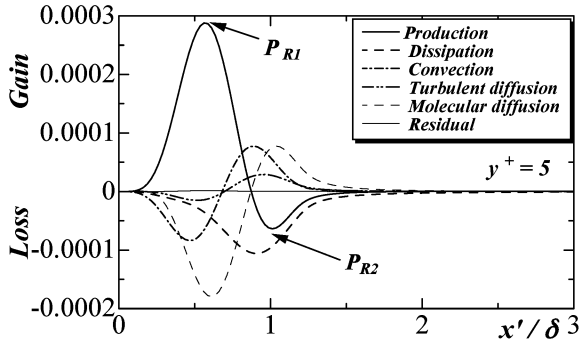

Figure 11: Budget of k_θ^*.

in Fig. 8 becomes indeed the molecular Prandtl number irrespective of the streamwise position. On the other hand, the obtained result in Fig. 8 has indicated that the time scale ratio varies along the streamwise direction in the outer region.

In the position of $x'/\delta = 0.4$, R is significantly higher than the unity at $y^+ = 4.3$ in Fig. 8. As can be seen from Fig. 9, it is due to the occurence of the peak in the temperature variance k_θ at $y^+ = 4.3$. Moreover, the local minimal value of its dissipation rate ε_θ is also observed at $y^+ = 4.3$ in Fig. 9. The local maximal values occur around $y^+ = 0$ and 7.5. This local maximums in ε_θ arise to dissipate the turbulent energy transported through molecular and turbulent diffusions from the peak in k_θ^* around $y^+ = 4$. The local minimal value of the dissipation rate exists at the peak of the temperature variance. Therefore, the peak of the time scale ratio occurs at $y^+ = 4.3$.

Figure 10 shows R at $y^+ = 5$, where an abscissa is assigned to the streamwise direction. It indicates that the time scale ratio varies along the streamwise direction. To examine the peak of both P_{R1} and P_{R2}, the budget for k_θ^* is shown in Fig. 11. The positions where the maximal and minimal peaks of the time scale ratio exist are in agreement with those of the production term P_{k_θ} for k_θ^*. In the case of the present streamwisely varying thermal boundary condition, P_{k_θ} is negative in latter half of the heated section. To explain the negative value of P_{k_θ}, the terms which constitute P_{k_θ} in the transport equation of k_θ^* are examined. Their expression and sign of the terms in the relevant region are

$$\begin{aligned} P_{k_\theta} &= \left(-\overline{u'^+\theta'^*}\frac{\partial \bar{T}^*}{\partial x}\right) + \left(-\overline{v'^+\theta'^*}\frac{\partial \bar{T}^*}{\partial y}\right) \\ &= (- \cdot - \cdot -) + (- \cdot + \cdot +) \\ &= \textit{negative}. \end{aligned} \tag{11}$$

The relation among $\overline{u'^+\theta'^*}$, $d\bar{T}^*/dx$, $\overline{v'^+\theta'^*}$, and $d\bar{T}^*/dy$ is seen in Figs. 4 and 5. In the position of the negative value of P_{k_θ}, $\overline{u'^+\theta'^*}$ and $d\bar{T}^*/dx$ stay negative and others positive value.

Figure 12 shows the two dimensional distribution of P_{k_θ}. The solid and dashed lines show the positive and negative values, respectively. The negative region of the production term occupies a fairly large area behind the heated section. This is because the hot fluid is convective from upstream, and thus the mean temperature gradient is inverted in the near-wall region. The two dimensional distribution of R is also shown in Fig. 13. There are one local maximum in the heated section and one local minimum in latter half of the heated section. A noticeable agreement in the profiles of P_{k_θ} and R is observed through the comparison of Figs. 12 and 13. The negative region of P_{k_θ} is in good agreement with that of the local minimum of R.

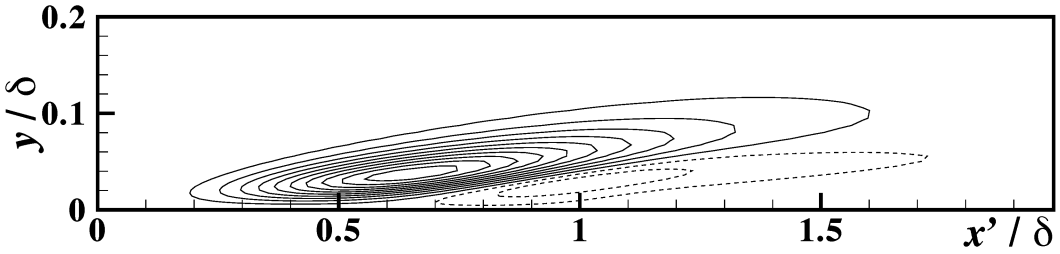

Figure 12: Side view of the production term P_{k_θ} for k_θ^*. Solid line are the positive value and dashed line are the negative one. Contour level is from -1.0×10^{-4} to 3.0×10^{-4} with increments of 5.0×10^{-5}.

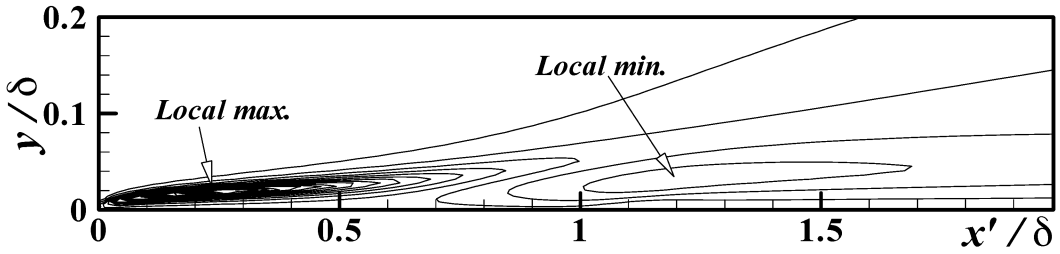

Figure 13: Side view of the time scale ratio R. Contour level is from 0.2 to 4 with increments of 0.2.

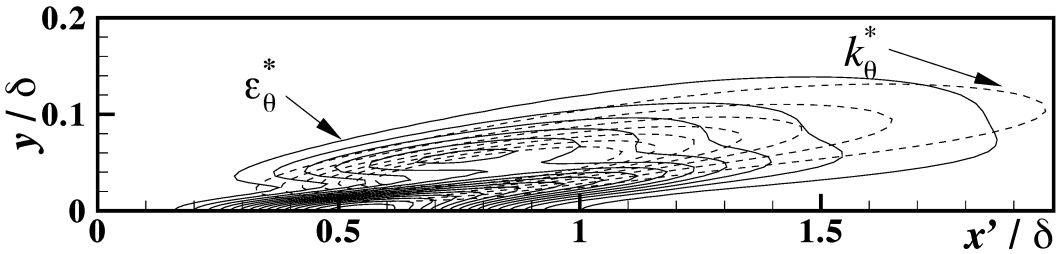

Figure 14: Side view of k_θ^* (dot line) and ε_θ^* (solid line). Contour level for k_θ^* is from 1.7×10^{-4} to 8.7×10^{-4} with increments of 1.0×10^{-4}, while that of ε_θ^* is from 1.1×10^{-6} to 1.7×10^{-4} with increments of 1.0×10^{-5}.

Figure 14 indicates the relation between the two dimensional profiles of k_θ and ε_θ is the same at any downstream position. It can be seen that the profiles of both k_θ and ε_θ are inclined toward the streamwise direction. One can notice that, in general, ε_θ is high where k_θ is large. More detailed inspection indicates that the contour of ε_θ possesses a large number of inflection points than that of k_θ. We have seen in Fig. 10 that the position of the local minimum in ε_θ corresponds to the maximum point of k_θ. This trend can be observed also in the two-dimensional contour of ε_θ, which causes the more complex profile of ε_θ than that of k_θ.

CONCLUSIONS

The DNS of turbulent heat transfer in a fully developed turbulent channel flow has been carried out for streamwisely varying thermal boundary condition with $Pr = 0.71$ and $Re_\tau = 180$ ($Re_c = 6600$). The thermal turbulence statistics such as the mean temperature, the turbulent heat flux, the temperature variance, its dissipation rate, the turbulent Prandtl number, and the time scale ratio have been discussed. These turbulence statistics significantly varies at the downstream position near the heated wall. In the streamwise and wall-normal turbulent heat flux, the interesting feature is that the counter gradient diffusion exists in both the latter half of the heated section and downstream. The observational evidence indicates that the region of the negative production term P_{k_θ} correlate well with the counter gradient diffusion. The time scale ratio also varies along the streamwise direction in the outer region. It results from the tendency that k_θ tends to decrease more rapidly than ε_θ in the near-wall region behind the heated section. Moreover, it has been confirmed that the local minimal value of ε_θ almost always exists at the peak of the temperature variance. This study indicates that the turbulent Prandtl number cannot be used for estimating the turbulent heat flux because it changes downstream remarkably due to the rapid variation in the thermal boundary condition.

ACKNOWLEDGEMENTS

This calculations were performed with the use of the VPP-5000 at Computing and Communications Center of Kyushu University, and also supercomputing resources at Information Synergy Center of Tohoku University.

REFERENCES

Abe, H., Kawamura, H. and Matsuo, Y., 2001, "Direct numerical simulation of a fully developed turbulent channel flow with respect to Reynolds number dependence", *ASME J. Fluids Eng.*, Vol. 123, pp. 382-393.

Antonia, R.A., Danh, H.Q. and Prabhu, A., 1977, "Response of a Turbulent Boundary Layer to a Step Change in Surface Heat Flux", *J. Fluid Mech.*, Vol. 80, pp. 153-177.

Antonia, R.A. & Kim, J., 1991, "Reynolds shear stress and heat flux calculations in a fully developed turbulent duct flow", *Int. J. Heat Mass Transfer*, Vol. 34, No. 8, pp. 2013-2018.

Johnson, D.S., 1959, "Velocity and Temperature Fluctuation Measurements in a Turbulent Boundary Layer Downstream of a Stepwise Discontinuity in Wall Temperature", *J. Appl. Mech., Trans. A.S.M.E.*, Vol. 26, pp. 325-336.

Kawamura, H., 1994, "Direct numerical simulation of turbulence by finite difference scheme", In: Zhang, Z. S. and Miyake, Y. (Eds.), The Recent Developments in Turbulence Research, International Academic Publishers, pp. 54-60.

Kawamura, H. and Kondoh, Y., 1996, "Application of consistent finite difference scheme to DNS of turbulent heat transfer in channel flow", *Proc. 3rd KSME/JSME Therm. Eng. Conf.*, Kyongju, Korea, Vol. 1, pp. 53-58.

Nagano, Y., Hattori, H. and Abe, K., 1995, "Modeling the Turbulent Heat and Momentum Transfer in Complex Flows under Various Thermal Conditions", *Proc. of Int. Symp. on Math. Modelling of Turbulent Flows*, Tokyo, Japan, pp. 79-86.

Seki, Y., Abe, H. and Kawamura, H., 2003, "DNS of turbulent heat transfer in a channel flow with different thermal boundary conditions", *Proc. 6th ASME/JSME Therm. Eng. Conf.*, USA, pp. 248.

Sreenivasan, K.R., Danh, H.Q. and Antonia, R.A., 1976, "Diffusion form a heated wall-cylinder immersed in a turbulent boundary layer", *Proc. of Thermaofluids Conf.*, Hobart, pp. 103-106.